On the Second Order Statistics of Cooperative UAV Communications underlying Interference Limited Composite Fading Conditions

Caslav Stefanovic*, Danijel Djosic†, Dusan Stefanovic‡, Hranislav Milosevic†, and Stefan R. Panic†
*Universidad Carlos III de Madrid, Department of Signal Theory and Communications, 28911 Leganés, Spain
Email: caslav.stefanovic@uc3m.es
†Faculty of Science and Mathematics, University of Pristina, Serbia,
Email: danijel.djosic@pr.ac.rs, hranislav.milosevic@pr.ac.rs, stefan.panic@pr.ac.rs
‡Collage of Applied Technical Sciences, Nis, Serbia Email: dusan.stefanovic@vts.edu.rs

***Abstract*—Unmanned-aerial-vehicles (UAVs) enabled communications (ECs) are intended to be an essential part of forthcoming beyond 5G (B5G) and 6G communication networks (CNs). UAV-to-ground (UG)-ECs in densely populated areas are usually exposed to composite fading conditions and the impact of co-channel interference (CCI). In this paper, we provide second order (SO)-metrics of UG communications over double-scattered, single-shadowed (DSc-SSh) fading channels in the interference limited environment, modeled as a ratio of the product of double $\alpha-\mu$ and Gamma (G) random variables (RVs). Novel integral form formulas for average fade duration (AFD) and level crossing rate (LCR) of the proposed UG communication system over the composite channels in the presence of CCI are efficiently obtained and approximated by Laplace based integration (LBI)-method. Moreover, the system model is extended to investigate the SO-metrics of cooperative UAV transmission selection (TS) system that chooses the UG transmission link with the highest signal level among L independent UG links. The impact of different DSc-SSh fading conditions as well as the number of UAVs on the SO-metrics are well addressed.**

***Index Terms*—Cooperative UAV communications, Composite fading, Interference limited environment, Second order statistics.**

I. Introduction

UAV-ECs is an important research topic within beyond 5G (B5G) and 6G communication networks (CNs) [1]-[3]. UAVs can be deployed in the air as base stations, relays, 3D mobile terminals and nodes for simultaneous wireless information and power transfer (SWIPT). Moreover, the B5G and 6G UAV-EC systems are applicable for radio-frequency (RF), millimeter wave, free space optical, visible light and terahertz communication technologies [4]-[8].

In order to efficiently enable various UAV-EC systems, accurate UG channel characterization and modeling is an important task [9]-[10]. The UG channel models based on measurements are provided in [11]. In urban scenarios coverage and path-loss due to buildings and other objects are occasionally difficult to predict. The UG communication systems in the presence of highly movable UAVs can be exposed to both line of sight (LOS) and non-LOS propagation conditions. Experimentally verified UG channels in urban areas can be modeled as double-scattered, single-shadowed (DSc-SSh) composite fading models [12]-[13]. Namely, [12]-[13] address first-order (FO)-metrics of UG system over DSc-SSh fading channels modeled as the product of independent double Nakagami-m (D-N) and single inverse Gamma (S-IG) random variables (RVs).

The major impairment in UG communications is co-channel interference (CCI), co-existing due to the ultra-dense CNs deployments [14]-[15]. Coverage probability and ergodic capacity of 3D UAV CN in the presence of CCI based on stochastic geometry are investigated in [16]. In [17], the impact of the interference on outage probability of UG communications is provided. An CCI aware path controlling scheme of cellular UAV CNs is considered in [18].

The SO-metrics can efficiently address system performances of UG systems in dynamic propagation conditions of rapidly time variant fading channels. In particular, the average level crossing rate (LCR) can be used to evaluate time rate of change of the UG signal envelope, while average fade duration (AFD) can be used to evaluate the mean time of the UG signal envelope being below a threshold.

The SO-metrics of a 3D non-stationary channels for UG communications are addressed in [19]-[20]. In [21], the SO-metrics of UAV-to-UAV (UU) and UG CNs are derived. The simulation and experimental SO-metrics for urban UG communications under fast-fading conditions are provided in [22]. The AFD of moving aerial base stations is considered in [23], while the impact of different operating frequencies on SO metrics for UG communications are addressed in [24]. The LCR and AFD of of UG system over DSc-SSh fading channels modeled as the product of independent D-N and S-IG RVs are addressed in [25]. However, the SO-metrics of UG systems in the presence of CCI have not been observed in the open literature so far.

This paper provides derivation of approximate closed form SO-metrics of a ratio of the product of double $\alpha-\mu$ and Gamma

978-1-6654-6975-3/22/$31.00 ©2022 IEEE

(G) RVs. The derived SO-metrics such as LCR and AFD are directly related to the performance of UG communications over DSc-SSh fading channels in urban areas. Moreover, the considered model is extended to include SO-metrics of cooperative TS system with L independent UG links.

II. System Model

The interference limited fading environments (when the impact of CCI is stronger than noise) can be modeled as a ratio of two random variables (RVs) [26]-[27]. Thus, the signal-to-interference (SIR) instantaneous power can be defined as

$$G_{out} = Z_{DS}^2 / Z_{CCI}^2 \tag{1}$$

whereas SIR envelope can be given as

$$Z_{out} = \sqrt{G_{out}} = Z_{DS} / Z_{CCI} \tag{2}$$

where Z_{DS} is a desired signal envelope and Z_{CCI} is a CCI envelope signal.

A. Composite DSc-SSh Fading Channels

The composite fading channels for UG communications can be modeled by experimentally tested double-scattered (DSc), single-shadowed (SSh) fading channels [12], [25]. In this paper, we model the desired DSc-SSh faded signal as the product of two α-μ RVs (denoted as $Z_{\alpha-\mu,1}$ and $Z_{\alpha-\mu,2}$) and one Gamma (G) RV (denoted as Z_{G_1}):

$$Z_{DS} = \underbrace{Z_{\alpha-\mu,1} Z_{\alpha-\mu,2}}_{DSc} \underbrace{Z_{G_1}}_{SSh} = \underbrace{Z_{N1}^{2/\alpha_1} Z_{N2}^{2/\alpha_2}}_{DSc} \underbrace{Z_{N3}^2}_{SSh} \tag{3}$$

where α-μ and G RVs can be expressed through Nakagami-m RVs as given in [28, Eq. (12)] and [29, Eq. (2.55)], respectively. In particular, $Z_{\alpha-\mu,i} = Z_{N,i}^{\frac{2}{\alpha_i}}, i = 1, 2$ and $Z_{G_1} = Z_{N,3}^2$. The α_i is a shaping parameter of $\alpha - \mu$ distribution. Moreover, the $\alpha - \mu$ is a well-known general distribution for multi-path signals composed of different clusters in a non-homogeneous propagation conditions [28], while double $\alpha - \mu$ distribution has been used in dynamic propagation conditions to describe double-scattered fading channels for vehicular systems [30]-[31]. The G distribution is experimentally tested and mathematically tractable fading model used to address shadowing in wireless communications [32]-[34]. Similarly, we define the CCI signal envelope originating from undesired source in DSc-SSh fading environment as

$$Z_{CCI} = \underbrace{Z_{\alpha-\mu,3} Z_{\alpha-\mu,4}}_{DSc} \underbrace{Z_{G_2}}_{SSh} = \underbrace{Z_{N4}^{2/\alpha_3} Z_{N5}^{2/\alpha_4}}_{DSc} \underbrace{Z_{N6}^2}_{SSh} \tag{4}$$

The PDFs of Nakagami-m RVs (denoted as $Z_{N,i}$, $i = 1, 6$) used to address Z_{DS} and Z_{CCI} are [29. Eq. (2.52)]:

$$p_{Z_{N,i}}(z_{N,i}) = \frac{2(\mu_i/\Omega_i)^{\mu_i}}{\Gamma(\mu_i)} (z_{N,i})^{2\mu_i - 1} e^{-\frac{\mu_i}{\Omega_i}(z_{N,i})^2}, i = 1, 6; \tag{5}$$

whose severity and shaping parameters are respectively, μ_i and Ω_i.

B. PDF of DSc-SSh SIR Envelope

The PDF of DSc-SSh SIR Envelope (denoted as Z_{out}) using (2)-(4) for the case when $\alpha = \alpha_1 = \alpha_2$ can be expressed as:

$$\begin{aligned} p_{Z_{out}}(z_{out}) &= \int_0^\infty dz_{N1} \int_0^\infty dz_{N2} \int_0^\infty dz_{N4} \int_0^\infty dz_{N5} \\ &\times \int_0^\infty |\frac{dz_{N3}}{dz_{out}}| p_{Z_{N1}}(z_{N1}) p_{Z_{N2}}(z_{N2}) p_{Z_{N4}}(z_{N4}) \\ &\times p_{Z_{N5}}(z_{N5}) p_{Z_{N6}}(z_{N6}) p_{Z_{N3}}(\frac{z_{out}^{\frac{1}{2}} z_{N4}^{\frac{\alpha}{2}} z_{N5}^{\frac{\alpha}{2}} z_{N6}}{z_{N_1}^{\frac{\alpha}{2}} z_{N_2}^{\frac{\alpha}{2}}}) dz_{N6} \end{aligned} \tag{6}$$

where $|\frac{dz_{N3}}{dz_{out}}| = \frac{\frac{1}{2} z_{out}^{-\frac{1}{2}} z_{N4}^{\frac{\alpha}{2}} z_{N5}^{\frac{\alpha}{2}} z_{N6}}{z_{N_1}^{\frac{\alpha}{2}} z_{N_2}^{\frac{\alpha}{2}}}$.

C. CDF of DSc-SSh SIR Envelope

The CDF of DSc-SSh SIR envelope for the considered UG link can be calculated by

$$F_{Z_{out}}(z_{out}) = \int_0^{z_{out}} p_{z_{out}}(s) ds \tag{7}$$

After introducing (5) in (6) and than (6) in (7) and by applying [35, Eq. (3.381.1)], [35, Eq. (8.352.1)] and [35, Eq. (3.471.9)], respectively, $F_{Z_{out}}(z_{out})$ for the case where m_3 is integer can be given as:

$$\begin{aligned} F_{Z_{out}}(z_{out}) &= \frac{32(\frac{\mu_1}{\Omega_1})^{\mu_1} (\frac{\mu_2}{\Omega_2})^{\mu_2} (\frac{\mu_4}{\Omega_4})^{\mu_4} (\frac{\mu_5}{\Omega_5})^{\mu_5} (\frac{\mu_6}{\Omega_6})^{\mu_6}}{\Gamma(\mu_1)\Gamma(\mu_2)\Gamma(\mu_3)\Gamma(\mu_4)\Gamma(\mu_5)\Gamma(\mu_6)} \\ &\times (\mu_3 - 1)! \left(\frac{\Gamma(\mu_1)\Gamma(\mu_2)\Gamma(\mu_4)\Gamma(\mu_5)\Gamma(\mu_6)}{32(\frac{\mu_1}{\Omega_1})^{\mu_1} (\frac{\mu_2}{\Omega_2})^{\mu_2} (\frac{\mu_4}{\Omega_4})^{\mu_4} (\frac{\mu_5}{\Omega_5})^{\mu_5} (\frac{\mu_6}{\Omega_6})^{\mu_6}} \right. \\ &\left. - \sum_{k=0}^{\mu_3 - 1} \frac{(\frac{\mu_3}{\Omega_3} z_{out}^2)^k}{k!} I_1 \right) \end{aligned} \tag{8}$$

where I_1 is 5-folded integral given as:

$$\begin{aligned} I_1 &= \int_0^\infty dz_{N1} \int_0^\infty dz_{N2} \int_0^\infty dz_{N4} \int_0^\infty dz_{N5} \\ &\times \int_0^\infty z_{N1}^{2\mu_1 - \frac{2}{a}k - 1} z_{N2}^{2\mu_2 - \frac{2}{a}k - 1} z_{N4}^{2\mu_4 + \frac{2}{a}k - 1} z_{N5}^{2\mu_5 + \frac{2}{a}k - 1} \\ &\times z_{N6}^{2\mu_6 + 2k - 1} e^{-\frac{\mu_1}{\Omega_1} z_{N1}^2 - \frac{\mu_2}{\Omega_2} z_{N2}^2 - \frac{\mu_3}{\Omega_3} (\frac{z_{out}^{\frac{1}{2}} z_{N4}^{\frac{\alpha}{2}} z_{N5}^{\frac{\alpha}{2}} z_{N6}}{z_{N_1}^{\frac{\alpha}{2}} z_{N_2}^{\frac{\alpha}{2}}})^2} \\ &\times e^{-\frac{\mu_4}{\Omega_4} z_{N4}^2 - \frac{\mu_5}{\Omega_5} z_{N5}^2 - \frac{\mu_6}{\Omega_6} z_{N6}^2} dz_{N6} \end{aligned} \tag{9}$$

The expression I_1 can be evaluated using Laplace based integration (LIB)-method for 5-folded integrals [36]-[38]. The closed form approximation of $F_{Z_{out}}(z_{out})$ can be evaluated by [37, Eq. (I.3)]:

$$\begin{aligned}&\int_0^\infty dz_{N1}\int_0^\infty dz_{N2}\int_0^\infty dz_{N4}\int_0^\infty dz_{N5}\int_0^\infty dz_{N6}\\&\times f_1(z_{N1},z_{N2},z_{N4},z_{N5},z_{N6})e^{-\gamma f_2(z_{N1},z_{N2},z_{N4},z_{N5},z_{N6})}\\&\approx(\frac{2\pi}{\gamma})^{\frac{5}{2}}\frac{f_1(z_{N10},z_{N20},z_{N40},z_{N50},z_{N60})}{\sqrt{detM}}\\&\times e^{-\gamma f_2(z_{N10},z_{N20},z_{N40},z_{N50},z_{N60})}\end{aligned}\tag{10}$$

where z_{N10}, z_{N20}, z_{N40}, z_{N50} and z_{N60} can be obtained by solving five differential equations,

$$\frac{\partial f_2(z_{N10},z_{N20},z_{N40},z_{N50},z_{N60})}{\partial z_{Ni0}}=0, i=1,2,4,5,6\tag{11}$$

The matrix M is given as (12) at the top of the next page.

The I_1 in (9) can be calculated by exponential LBI-method for the following set of functions: γ=1, $f_1=1$,

$$\begin{aligned}f_2=&\frac{\mu_1}{\Omega_1}z_{N1}^2+\frac{\mu_2}{\Omega_2}z_{N2}^2+\frac{\mu_3}{\Omega_3}(\frac{z_{out}^{\frac{1}{2}}z_{N_4}^{\frac{\alpha}{2}}z_{N_5}^{\frac{\alpha}{2}}z_{N_6}}{z_{N_1}^{\frac{\alpha}{2}}z_{N_2}^{\frac{\alpha}{2}}})^2+\frac{\mu_4}{\Omega_4}z_{N4}^2\\&+\frac{\mu_5}{\Omega_5}z_{N5}^2+\frac{\mu_6}{\Omega_6}z_{N6}^2-(2\mu_1-\frac{2}{a}k-1)lnz_{N1}\\&-(2\mu_2-\frac{2}{a}k-1)lnz_{N2}-(2\mu_4+\frac{2}{a}k-1)lnz_{N4}\\&-(2\mu_5+\frac{2}{a}k-1)lnz_{N5}-(2\mu_6+2k-1)lnz_{N6}\end{aligned}\tag{13}$$

By substituting (13) in (11), we derived $z_{N10}, z_{N20}, z_{N40}, z_{N50}$ and z_{N50} and than after introducing (12) and (13) in respect to $z_{N10}, z_{N20}, z_{N40}, z_{N50}$ and z_{N50} in (10), the I_1 in (9) is calculated as a closed form expression.

D. LCR of DSc-SSh SIR Envelope

The LCR for a predetermined threshold z_{th}, denoted as $LCR_{out}(z_{th})$ is defined as:

$$LCR_{out}(z_{th})=\int_0^\infty \dot{z}_{out}p_{z_{out}\dot{z}_{out}}(z_{th}\dot{z}_{out})d\dot{z}_{out}\tag{14}$$

where $\dot{z}_{out}$ is the first derivative of z_{out}. The $p_{Z_{out}\dot{Z}_{out}}(z_{out}\dot{z}_{out})$ can be evaluated by averaging the joint PDF of independent RVs, $z_{out}, \dot{z}_{out}, z_{N1}, z_{N2}$,$z_{N4}$,$z_{N5}$ and z_{N6} [37, Eq. (12)]:

$$\begin{aligned}p_{Z_{out}\dot{Z}_{out}}(z_{out}\dot{z}_{out})=&\int_0^\infty dz_{N1}\int_0^\infty dz_{N2}\int_0^\infty dz_{N4}\\&\times\int_0^\infty dz_{N5}\int_0^\infty p_{Z_{out}\dot{Z}_{out}Z_{N1}Z_{N2}Z_{N4}Z_{N5}Z_{N6}}dz_{N6}\end{aligned}\tag{15}$$

where $p_{Z_{out}\dot{Z}_{out}Z_{N1}Z_{N2}Z_{N4}Z_{N5}Z_{N6}}$ can be transformed as [37, Eq. (13)]:

$$\begin{aligned}&p_{Z_{out}\dot{Z}_{out}Z_{N1}Z_{N2}Z_{N4}Z_{N5}Z_{N6}}\\&=p_{\dot{Z}_{out}|Z_{out}Z_{N1}Z_{N2}Z_{N4}Z_{N5}Z_{N6}}p_{Z_{out}|Z_{N1}Z_{N2}Z_{N4}Z_{N5}Z_{N6}}\\&\times p_{Z_{N1}}p_{Z_{N2}}p_{Z_{N4}}p_{Z_{N5}}p_{Z_{N6}}\end{aligned}\tag{16}$$

where,

$$p_{Z_{out}|Z_{N1}Z_{N2}Z_{N4}Z_{N5}Z_{N6}}=|\frac{dz_{N3}}{dz_{out}}|p_{z_{N3}}(\frac{z_{out}^{\frac{1}{2}}z_{N_4}^{\frac{\alpha}{2}}z_{N_5}^{\frac{\alpha}{2}}z_{N_6}}{z_{N_1}^{\frac{\alpha}{2}}z_{N_2}^{\frac{\alpha}{2}}})\tag{17}$$

After substitutions, (17) in (16), (16) in (15) and (15) in (14), respectively, the $LCR_{out}(z_{th})$ becomes:

$$\begin{aligned}LCR_{out}(z_{th})=&\int_0^\infty dz_{N1}\int_0^\infty dz_{N2}\int_0^\infty dz_{N4}\int_0^\infty dz_{N5}\\&\times\int_0^\infty|\frac{dz_{N3}}{dz_{out}}|p_{z_{N3}}(\frac{z_{out}^{\frac{1}{2}}z_{N_4}^{\frac{\alpha}{2}}z_{N_5}^{\frac{\alpha}{2}}z_{N_6}}{z_{N_1}^{\frac{\alpha}{2}}z_{N_2}^{\frac{\alpha}{2}}})p_{Z_{N1}}(z_{N1})\\&\times p_{Z_{N2}}(z_{N2})p_{Z_{N4}}(z_{N4})p_{Z_{N5}}(z_{N5})p_{Z_{N6}}(z_{N6})dz_{N6}\\&\times\int_0^\infty\dot{z}_{out}p_{\dot{z}_{out}|Z_{out}Z_{N1}Z_{N2}Z_{N3}Z_{N5}Z_{N6}}d\dot{z}_{out}\end{aligned}\tag{18}$$

where $\int_0^\infty \dot{z}_{out}p_{\dot{Z}_{out}|Z_{out}Z_{N1}Z_{N2}Z_{N3}Z_{N5}Z_{N6}}=\frac{1}{\sqrt{2\pi}}\sigma_{\dot{z}_{out}}$. The first derivative of the z_{out} can be expressed as:

$$\begin{aligned}\dot{z}_{out}=&\frac{\frac{\alpha}{2}z_{N1}^{\frac{\alpha}{2}-1}z_{N_2}^{\frac{\alpha}{2}}z_{N_3}\dot{z}_{N1}}{z_{N_4}^{\frac{\alpha}{2}}z_{N_5}^{\frac{\alpha}{2}}z_{N_6}}+\frac{\frac{\alpha}{2}z_{N1}^{\frac{\alpha}{2}}z_{N_2}^{\frac{\alpha}{2}-1}z_{N_3}\dot{z}_{N2}}{z_{N_4}^{\frac{\alpha}{2}}z_{N_5}^{\frac{\alpha}{2}}z_{N_6}}\\&+\frac{z_{N1}^{\frac{\alpha}{2}}z_{N_2}^{\frac{\alpha}{2}}\dot{z}_{N3}}{z_{N_4}^{\frac{\alpha}{2}}z_{N_5}^{\frac{\alpha}{2}}z_{N_6}}-\frac{\alpha}{2}\frac{z_{N1}^{\frac{\alpha}{2}}z_{N_2}^{\frac{\alpha}{2}}z_{N_3}\dot{z}_{N4}}{z_{N_4}^{\frac{\alpha}{2}+1}z_{N_5}^{\frac{\alpha}{2}}z_{N_6}}\\&-\frac{\alpha}{2}\frac{z_{N1}^{\frac{\alpha}{2}}z_{N_2}^{\frac{\alpha}{2}}z_{N_3}\dot{z}_{N5}}{z_{N_4}^{\frac{\alpha}{2}}z_{N_5}^{\frac{\alpha}{2}+1}z_{N_6}}-\frac{z_{N1}^{\frac{\alpha}{2}}z_{N_2}^{\frac{\alpha}{2}}z_{N_3}\dot{z}_{N6}}{z_{N_4}^{\frac{\alpha}{2}}z_{N_5}^{\frac{\alpha}{2}}z_{N_6}^2}\end{aligned}\tag{19}$$

where $\dot{z}_{N1}, \dot{z}_{N2}, \dot{z}_{N3}$, $\dot{z}_{N4}$, $\dot{z}_{N5}$ and $\dot{z}_{N6}$ are the first derivatives of z_{N1}, z_{N2}, z_{N3}, z_{N4}, z_{N5} and z_{N6}, respectively. Since the linear transformation of zero mean Gaussian (Z-M-G) RVs is a Z-M-G RV, the variance of $\dot{z}_{out}$ is also a Z-M-G RV and $\sigma^2_{\dot{z}_{out}}$ can be expressed through the variances of $\dot{z}_{N1}, \dot{z}_{N2}, \dot{z}_{N3}$, $\dot{z}_{N4}$, $\dot{z}_{N5}$ and $\dot{z}_{N6}$ expressed as $\sigma^2_{\dot{z}_{N1}}, \sigma^2_{\dot{z}_{N2}}$, $\sigma^2_{\dot{z}_{N3}}$, $\sigma^2_{\dot{z}_{N4}}$, $\sigma^2_{\dot{z}_{N5}}$ and $\sigma^2_{\dot{z}_{N6}}$, respectively:

$$\begin{aligned}\sigma^2_{\dot{z}_{out}}=&\frac{4z_{out}^2}{\alpha^2z_{N1}^2}\sigma^2_{\dot{z}_{N1}}(1+\frac{z_{N1}^2}{z_{N2}^2}\sigma^2_{\dot{z}_{N2}}/\sigma^2_{\dot{z}_{N1}}\\&+\alpha^2\frac{z_{N1}^{2/\alpha+2}z_{N2}^{2/\alpha}}{z_{out}z_{N4}^{2/\alpha}z_{N5}^{2/\alpha}z_{N6}^2}\sigma^2_{\dot{z}_{N3}}/\sigma^2_{\dot{z}_{N1}}+\frac{z_{N1}^2}{z_{N4}^2}\sigma^2_{\dot{z}_{N4}}/\sigma^2_{\dot{z}_{N1}}\\&+\frac{z_{N1}^2}{z_{N5}^2}\sigma^2_{\dot{z}_{N5}}/\sigma^2_{\dot{z}_{N1}}+\alpha^2\frac{z_{N1}^2}{z_{N6}^2}\sigma^2_{\dot{z}_{N6}}/\sigma^2_{\dot{z}_{N1}})\end{aligned}\tag{20}$$

$$M = \begin{bmatrix} \frac{\partial^2 f_2}{\partial z_{N10}^2} & \frac{\partial^2 f_2}{\partial z_{N10}\partial z_{N20}} & \frac{\partial^2 f_2}{\partial z_{N10}\partial z_{N40}} & \frac{\partial^2 f_2}{\partial z_{N10}\partial z_{N50}} & \frac{\partial^2 f_2}{\partial z_{N10}\partial z_{N60}} \\ \frac{\partial^2 f_2}{\partial z_{N20}\partial z_{N10}} & \frac{\partial^2 f_2}{\partial z_{N20}^2} & \frac{\partial^2 f_2}{\partial z_{N20}\partial z_{N40}} & \frac{\partial^2 f_2}{\partial z_{N20}\partial z_{N50}} & \frac{\partial^2 f_2}{\partial z_{N20}\partial z_{N60}} \\ \frac{\partial^2 f_2}{\partial z_{N40}\partial z_{N10}} & \frac{\partial^2 f_2}{\partial z_{N40}\partial z_{N20}} & \frac{\partial^2 f_2}{\partial z_{N40}^2} & \frac{\partial^2 f_2}{\partial z_{N40}\partial z_{N50}} & \frac{\partial^2 f_2}{\partial z_{N40}\partial z_{N60}} \\ \frac{\partial^2 f_2}{\partial z_{N50}\partial z_{N10}} & \frac{\partial^2 f_2}{\partial z_{N50}\partial z_{N20}} & \frac{\partial^2 f_2}{\partial z_{N50}\partial z_{N40}} & \frac{\partial^2 f_2}{\partial z_{N50}^2} & \frac{\partial^2 f_2}{\partial z_{N50}\partial z_{N60}} \\ \frac{\partial^2 f_2}{\partial z_{N60}\partial z_{N10}} & \frac{\partial^2 f_2}{\partial z_{N60}\partial z_{N20}} & \frac{\partial^2 f_2}{\partial z_{N60}\partial z_{N40}} & \frac{\partial^2 f_2}{\partial z_{N60}\partial z_{N50}} & \frac{\partial^2 f_2}{\partial z_{N60}^2} \end{bmatrix} \tag{12}$$

Lastly, the $LCR_{out}(z_{th})$ can be given as:

$$LCR_{out}(z_{th}) = \frac{32\sigma_{\dot{x}_{N1}}^2 (\frac{\mu_1}{\Omega_1})^{\mu_1} (\frac{\mu_2}{\Omega_2})^{\mu_2} (\frac{\mu_3}{\Omega_3})^{\mu_3} (\frac{\mu_4}{\Omega_4})^{\mu_4}}{\sqrt{2\pi}\Gamma(\mu_1)\Gamma(\mu_2)\Gamma(\mu_3)\Gamma(\mu_4)} \times \frac{(\frac{\mu_5}{\Omega_5})^{\mu_5} (\frac{\mu_6}{\Omega_6})^{\mu_6}}{\Gamma(\mu_5)\Gamma(\mu_6)} z_{th}^{2\mu_1-1} I_2 \tag{21}$$

where I_2 is

$$\begin{aligned} I_2 = & \int_0^\infty dz_{N1} \int_0^\infty dz_{N2} \int_0^\infty dz_{N4} \int_0^\infty dz_{N5} \int_0^\infty dz_{N6} \\ & \times (1 + \frac{z_{N1}^2}{z_{N2}^2}\sigma_{\dot{z}_{N2}}^2/\sigma_{\dot{z}_{N1}}^2 + \alpha^2 \frac{z_{N1}^{2/\alpha+2} z_{N2}^{2/\alpha}}{z_{out} z_{N4}^{2/\alpha} z_{N5}^{2/\alpha} z_{N6}^2}\sigma_{\dot{z}_{N3}}^2/\sigma_{\dot{z}_{N1}}^2 \\ & + \frac{z_{N1}^2}{z_{N4}^2}\sigma_{\dot{z}_{N4}}^2/\sigma_{\dot{z}_{N1}}^2 + \frac{z_{N1}^2}{z_{N5}^2}\sigma_{\dot{z}_{N5}}^2/\sigma_{\dot{z}_{N1}}^2 + \alpha^2 \frac{z_{N1}^2}{z_{N6}^2}\sigma_{\dot{z}_{N6}}^2/\sigma_{\dot{z}_{N1}}^2)^{1/2} \\ & \times z_{N1}^{2\mu_1 - \frac{2}{a}\mu_3 - 2} z_{N2}^{2\mu_2 - \frac{2}{a}\mu_3 - 1} z_{N4}^{2\mu_4 + \frac{2}{a}\mu_3 - 1} z_{N5}^{2\mu_5 + \frac{2}{a}\mu_3 - 1} \\ & \times z_{N6}^{2\mu_6 + 2\mu_3 - 1} e^{-\frac{\mu_1}{\Omega_1} z_{N1}^2 - \frac{\mu_2}{\Omega_2} z_{N2}^2 - \frac{\mu_3}{\Omega_3} (\frac{z_{out}^{\frac{1}{2}} z_{N4}^{\frac{\alpha}{2}} z_{N5}^{\frac{\alpha}{2}} z_{N6}}{z_{N1}^{\frac{\alpha}{2}} z_{N2}^{\frac{\alpha}{2}}})^2} \\ & \times e^{-\frac{\mu_4}{\Omega_4} z_{N4}^2 - \frac{\mu_5}{\Omega_5} z_{N5}^2 - \frac{\mu_6}{\Omega_6} z_{N6}^2} \end{aligned} \tag{22}$$

The I_2 can be solved by LBI-method, already provided by (10), (11) and (12) for the following γ, $f_1(z_{N1}, z_{N2}, z_{N4}, z_{N5}, z_{N6})$ and $f_2(z_{N1}, z_{N2}, z_{N4}, z_{N5}, z_{N6})$, respectively: γ=1,

$$\begin{aligned} f_1 = & (1 + \frac{z_{N1}^2}{z_{N2}^2}\sigma_{\dot{z}_{N2}}^2/\sigma_{\dot{z}_{N1}}^2 + \alpha^2 \frac{z_{N1}^{2/\alpha+2} z_{N2}^{2/\alpha}}{z_{out} z_{N4}^{2/\alpha} z_{N5}^{2/\alpha} z_{N6}^2}\sigma_{\dot{z}_{N3}}^2/\sigma_{\dot{z}_{N1}}^2 \\ & + \frac{z_{N1}^2}{z_{N4}^2}\sigma_{\dot{z}_{N4}}^2/\sigma_{\dot{z}_{N1}}^2 + \frac{z_{N1}^2}{z_{N5}^2}\sigma_{\dot{z}_{N5}}^2/\sigma_{\dot{z}_{N1}}^2 + \alpha^2 \frac{z_{N1}^2}{z_{N6}^2}\sigma_{\dot{z}_{N6}}^2/\sigma_{\dot{z}_{N1}}^2)^{1/2} \end{aligned} \tag{23}$$

$$\begin{aligned} f_2 = & \frac{\mu_1}{\Omega_1} z_{N1}^2 + \frac{\mu_2}{\Omega_2} z_{N2}^2 + \frac{\mu_3}{\Omega_3} (\frac{z_{out}^{\frac{1}{2}} z_{N4}^{\frac{\alpha}{2}} z_{N5}^{\frac{\alpha}{2}} z_{N_6}}{z_{N_1}^{\frac{\alpha}{2}} z_{N_2}^{\frac{\alpha}{2}}})^2 + \frac{\mu_4}{\Omega_4} z_{N4}^2 \\ & + \frac{\mu_5}{\Omega_5} z_{N5}^2 + \frac{\mu_6}{\Omega_6} z_{N6}^2 - (2\mu_1 - \frac{2}{a}\mu_3 - 2) ln z_{N1} \\ & - (2\mu_2 - \frac{2}{a}\mu_3 - 1) ln z_{N2} - (2\mu_4 + \frac{2}{a}\mu_3 - 1) ln z_{N4} \\ & - (2\mu_5 + \frac{2}{a}\mu_3 - 1) ln z_{N5} - (2\mu_6 + 2\mu_3 - 1) ln x_{N6} \end{aligned} \tag{24}$$

Similarly, the $z_{N10}, z_{N20}, z_{N40}, z_{N50}$ and z_{N50} for this particular case are obtained by substituting (24) in (11) and than by substituting (23) and (24) in (10), approximate closed form $LCR_{out}(z_{th})$ is derived.

E. AFD of DSc-SSh SIR Envelope

The average fade duration (AFD) for a predetermined threshold z_{TH}, denoted as $AFD_{out}(z_{th})$ can be derived as:

$$AFD_{out}(z_{th}) = \frac{F_{out}(z_{th})}{LCR_{out}(z_{th})} \tag{25}$$

F. Cooperative UAV Communications

The considered system model is further extended to consider L transmission UG links that selects the UG link with the highest SIR envelope level. The CDF of SIR envelope for cooperative transmission selection (TS) UG system model over DSc-SSh fading, denoted as $F_X^{(S)}(x)$ can be expressed as:

$$F_{out}^{(TS)}(z) = F_{out}(z_{out})^L \tag{26}$$

LCR of SIR envelope with the UG transmission selection over DSc-SSh fading can be evaluated as:

$$LCR_{out}^{(TS)}(z_{th}) = L \times LCR_{out}(z_{th}) F_{out}(z_{th})^{L-1} \tag{27}$$

Lastly, the $AFD_{out}^{(TS)}(z_{th})$ or SIR envelope over DSc-SSh channel with UAV selection is:

$$AFD_{out}^{(TS)}(z_{th}) = \frac{F_{out}(z_{th})}{L \times LCR_{out}(z_{th})} \tag{28}$$

III. Numerical Results

The SO-metrics of UG communications as well as cooperative UG communications with TS over DSc-SSh channels are numerically evaluated for $\Omega_i = 1$ and presented for different system parameters on Fig. 1-4. The variances in (20) are expressed as $\sigma^2_{\dot{z}_{Ni}} = \pi^2 f^2_{\mu_i} \frac{\Omega_i}{\mu_i}, i = 1, 6$ where the maximum Doppler frequencies are assumed to be the same [37, Eq. (43)], $f_m = f_{m_i} = \sqrt{f^2_{m_{Tz}} + f^2_{m_{Rz}}}$, whereas $f_{m_{Tz}}$ and $f_{m_{Rz}}$ are maximal Doppler frequencies of the UAV transmitter and the ground receiver, respectively. The presented results on Fig 1-2 show that exact analytical expression (integral form expression) for $LCR_{out}(z_{th})/\sigma_{\dot{x}_{N1}}$ and $AFD_{out}(z_{th}) \times \sigma_{\dot{x}_{N1}}$ for the observed thresholds fit well with the approximation (closed form expressions approximated by LBI-method), especially for higher threshold values. Fig. 3 shows normalized $LCR^{(TS)}_{out}(z_{th})/f_m$. The increasing number of independent UG links causes $LCR^{(TS)}_{out}(z_{th})/f_m$ values to decrease for lower z_{th}. It can be seen further that by increasing all DSc-SSh severity parameters (μ_i) and non-homogeneity parameter (α), $LCR^{(TS)}_{out}(z_{th})$ decreases in the whole observable z_{TH} dB regime, which in turn can enable SO performance improvement. Moreover, it can be observed that the number of available UG links have stronger impact on $LCR^{(TS)}_{out}(z_{th})$ than DSc-SSh severity conditions for lower dB z_{th} values. The behavior of $AFD^{(TS)}_{out}(z_{th})$ multiplied by f_m is provided in Fig. 4. The graph show that by increasing all DSc-SSh severity parameters and non-homogeneity parameters, $AFD^{(TS)}_{out}(z_{th})f_m$ slightly decreases in lower z_{TH} threshold dB regime while $AFD^{(TS)}_{out}(z_{th})f_m$ increases in higher z_{th} dB regime. It is evident that increasing number of UG links can significantly improve the system performance, since $AFD^{(TS)}_{out}(z_{th})f_m$ decreases in whole z_{th} output regime. Moreover, the impact of the number of available independent UG links on $AFD^{(TS)}_{out}(z_{th})f_m$ is stronger than DSc-SSh fading conditions.

IV. Conclusion

The SO-metrics of SIR based cooperative UG communications in urban areas over DSc-SSh fading channels are considered. Namely, we provide formulas for the SO-metrics of the ratio of the product of double $\alpha - \mu$ and gamma RVs. The LBI-method has been used for derivation of closed form approximate SO-metrics. In particular, a less severe DSc-SSh multipath and shadowing conditions can provide system performance improvement for lower dB threshold values. Moreover, the increasing number of available independent UG links can significantly improve the system performance of considered selective cooperative UG system.

Acknowledgment

Acknowledgment to the CONEX-Plus that has received funding from UC3M and the EU's Horizon 2020 programme under the Marie Skłodowska-Curie grant No 801538.

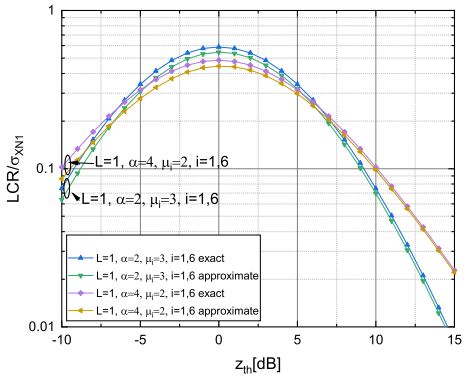

Fig. 1. LCR_{out} of SIR envelope divided by $\sigma_{\dot{x}_{N1}}$ versus z_{th} for single UG link over DSc-SSh channels under different parameters.

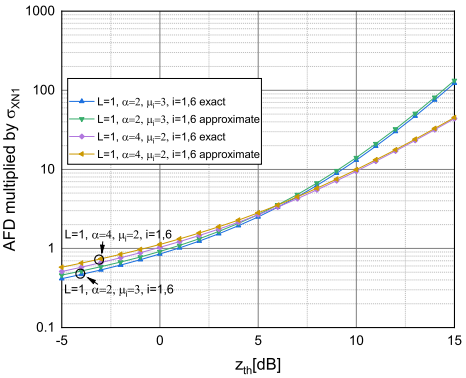

Fig. 2. AFD_{out} of SIR envelope multiplied by $\sigma_{\dot{x}_{N1}}$ versus z_{th} for single UG link over DSc-SSh channels under different parameters.

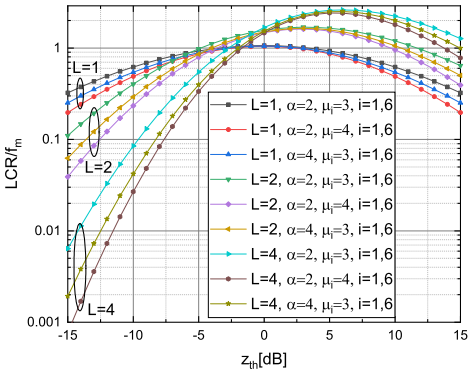

Fig. 3. $LCR^{(TS)}_{out}$ of SIR envelope divided by f_m versus z_{th} for cooperative UG communications over DSc-SSh channels under different parameters.

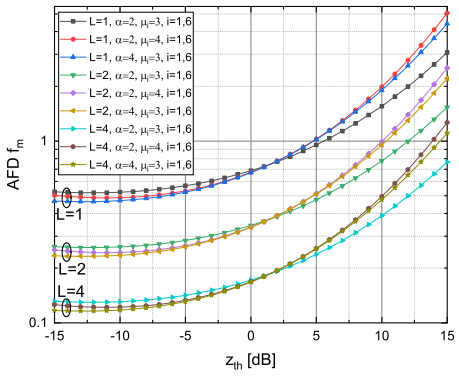

Fig. 4. $AFD_{out}^{(TS)}$ of SIR envelope multiplied by f_m versus z_{th} for cooperative UG communications over DSc-SSh channels under different parameters.

REFERENCES

[1] A. Masaracchia, et al., "UAV-enabled ultra-reliable low-latency communications for 6G: A comprehensive survey." IEEE Access, 2021.

[2] G. Geraci, et al. "What will the future of UAV cellular communications be? A flight from 5G to 6G", arXiv preprint arXiv:2105.04842,2021.

[3] S. Panic, C. Stefanovic, "UAV-Assisted Wireless Power Sensor Networks." In Integration of Unmanned Aerial Vehicles in Wireless Communication and Networks, pp. 61-77. Springer, Cham, 2023.

[4] P. K. Singya, M. S. Alouini, "Performance of UAV-Assisted Multiuser Terrestrial-Satellite Communication System Over Mixed FSO/RF Channels", IEEE Transactions on Aerospace and Electronic Systems, vol. 58, no. 2, pp. 781-796, 2021.

[5] S. Panic, T. D. P. Perera, et al., "UAV-assited wireless powered sensor network over Rician shadowed fading channels", *IEEE International Conference on Microwaves, Antennas, Communications and Electronic Systems (COMCAS)*, 2019.

[6] W. Yi, et al., "A unified spatial framework for UAV-aided mmWave networks," IEEE Transactions on Communications, vol. 67, no. 12, pp. 8801-8817, 2019.

[7] Y. Yang, et al., "Power efficient visible light communication with unmanned aerial vehicles," IEEE Communications Letters, vol. 23, no. 7, pp. 1272-1275, 2019.

[8] Y. Pan, et al., "UAV-assisted and intelligent reflecting surfaces-supported terahertz communications", IEEE Wireless Communications Letters, vol. 10, no. 6, pp. 1256-1260, 2021.

[9] W. Khawaja, et al., "A survey of air-to-ground propagation channel modeling for unmanned aerial vehicles." IEEE Communications Surveys Tutorials, vol. 21, no. 3, pp. 2361-2391, 2021.

[10] C. Yan, et al. "A comprehensive survey on UAV communication channel modeling." IEEE Access, vol. 7, pp. 107769-107792, 2019.

[11] W. Khawaja, et al., "UWB air-to-ground propagation channel measurements and modeling using UAVs", In 2019 IEEE Aerospace Conference (pp. 1-10). IEEE, 2019.

[12] P. S. Bithas et al., "UAV-to-ground communications: Channel modeling and UAV selection," IEEE Trans. Commun., vol. 68, no. 8, pp. 5135–5144, Aug. 2020.

[13] D. Dixit et al., "On the ASER Performance of UAV-Based Communication Systems for QAM Schemes," in IEEE Communications Letters, vol. 25, no. 6, pp. 1835-1838, June 2021.

[14] W. Mei, Q. Wu, and R. Zhang. "Cellular-connected UAV: Uplink association, power control and interference coordination" IEEE Transactions on wireless communications, vol. 18, no. 11, pp. 5380-5393, 2019.

[15] W. Mei, R. Zhang, "Aerial-ground interference mitigation for cellular-connected UAV", IEEE Wireless Communications, vol. 28, no. 1, pp. 167-173, 2021.

[16] C. K. Armeniakos, P. S. Bithas and A. G. Kanatas "SIR Analysis in 3D UAV Networks: A Stochastic Geometry Approach," *IEEE Access*, vol. 8, pp. 204963-204973, 2020.

[17] M. Kim, J. Lee, "Impact of an interfering node on unmanned aerial vehicle communications", IEEE Transactions on Vehicular Technology, vol. 68, no. 12, pp. 12150-12163, 2019.

[18] U. Challita, et al., "Interference management for cellular-connected UAVs: A deep reinforcement learning approach", IEEE Transactions on Wireless Communications, vol. 18, no. 4, pp. 2125-2140, 2019.

[19] Q. Zhu, et al., "Envelope Level Crossing Rate and Average Fade Duration of a Generic 3D Non-Stationary UAV Channel Model," *IEEE Access*, vol. 8, pp. 143134–143143, 2020.

[20] X. Zhang and X. Cheng "Second Order Statistics of Simulation Models for UAV-MIMO Ricean Fading Channels," *In ICC 2019-2019 IEEE International Conference on Communications (ICC)*, pp. 1–6, 2019.

[21] F. Jameel, et al., "Second order fading statistics of UAV networks," *In 2017 Fifth International Conference on Aerospace Science & Engineering (ICASE)*, pp. 1–6, 2017.

[22] M. Simunek, et al., "Space diversity gain in urban area low elevation links for surveillance applications," *IEEE Transactions on Antennas and Propagation*, vol. 61, no. 7, pp. 3850–3858, 2013.

[23] S. Enayati, et al., "Moving aerial base station networks: A stochastic geometry analysis and design perspective," *IEEE Transactions on Wireless Communications*, vol. 18, no. 6, pp. 2977–2988, 2019.

[24] Z. Cui, et al., "Multi-Frequency Air-to-Ground Channel Measurements and Analysis for UAV Communication Systems," *IEEE Access*, vol. 8, pp. 110565–110574, 2020.

[25] C. Stefanovic et al., "On Second-Order Statistics of the Composite Channel Models for UAV-to-Ground Communications With UAV Selection," in IEEE Open Journal of the Communications Society, vol. 2, pp. 534-544, 2021.

[26] J. F. Paris, "Outage probability in $\eta-\mu/\eta-\mu$ and $\kappa-\mu/\eta-\mu$ interference-limited scenarios", IEEE Transactions on Communications, vol. 61, no. 1, pp. 335-343,2012.

[27] N. Milosevic, et al., "Performance analysis of interference-limited mobile-to-mobile κ–μ fading channel", *Wireless Personal Communications*, vol, 101, no. 3, pp. 1685-1701, 2018.

[28] M. D. Yacoub, "The α-μ Distribution: A Physical Fading Model for the Stacy Distribution," in IEEE Transactions on Vehicular Technology, vol. 56, no. 1, pp. 27-34, Jan. 2007.

[29] L. G. Stuber, *Principles of mobile communication*, Norwell, Mass, USA: Kluwer Academic, 1996.

[30] P. Bithas, et al., "On the double-generalized gamma statistics and their application to the performance analysis of V2V communications", *IEEE Transactions on Communications*, vol. 66, no. 1, pp. 448–460, 2017.

[31] V. K. Chapala, et al., "RIS-Assisted Vehicular Network with Direct Transmission over Double-Generalized Gamma Fading Channels", arXiv preprint arXiv:2204.09958, 2022.

[32] I. M. Kostić, "Analytical approach to performance analysis for channel subject to shadowing and fading", *IEE Proceedings-Communications*, vol. 156, no. 6, pp. 821–827, 2005.

[33] H. Al-Hmood and H. S. Al-Raweshidy, "Unified Modeling of Composite $\kappa-\mu$/Gamma, $\eta-\mu$/Gamma, and $\alpha-\mu$/Gamma Fading Channels Using a Mixture Gamma Distribution With Applications to Energy Detection", *IEEE Antennas and Wireless Propagation Letters*, vol. 16, pp. 104-108, 2016.

[34] S. Suljović, et al. "Level crossing rate of macro diversity reception in composite Nakagami-m and Gamma fading environment with interference", Digital Signal Processing, no. 102, pp. 102758, 2020.

[35] I. S. Gradshteyn and I. M. Ryzhik, *Table of Integrals, Series, and Products*, New York: Academic, 2000.

[36] R. Butler and A. T. A. Wood, "Laplace Approximations for Hypergeometric Functions of Matrix Argument", *The Annals of Statistics*, vol. 30, pp. 1155–1177, 2001.

[37] Z. Hadzi-Velkov, et al., "On the second order statistics of the multihop Rayleigh fading channel", *IEEE Transactions on Communications*, vol. 57, no. 6, pp. 1815–1823, 2009.

[38] C. Stefanovic et al., "On the second order statistics of N-hop FSO communications over N-gamma-gamma turbulence induced fading channels," *Physical Communication*, p.101289, 2021.